

Nonlinear mixing-based terahertz emission in inclined rippled density plasmas

K Gopal, A P Singh, and S Divya

Citation: Chin. Phys. B, 2023, 32 (**6**): 065202. DOI: 10.1088/1674-1056/aca9c9
Journal homepage: http://cpb.iphy.ac.cn; http://iopscience.iop.org/cpb

What follows is a list of articles you may be interested in

Intense low-noise terahertz generation by relativistic laser irradiating near-critical-density plasma

Shijie Zhang(张世杰), Weimin Zhou(周维民), Yan Yin(银燕), Debin Zou(邹德滨), Na Zhao(赵娜), Duan Xie(谢端), and Hongbin Zhuo(卓红斌)
Chin. Phys. B, 2023, 32 (**3**): 035201. DOI: 10.1088/1674-1056/ac872c

Propagation of terahertz waves in nonuniform plasma slab under "electromagnetic window"

Hao Li(李郝), Zheng-Ping Zhang(张正平), and Xin Yang (杨鑫)
Chin. Phys. B, 2022, 31 (**3**): 035202. DOI: 10.1088/1674-1056/ac1b90

Suppression of auto-resonant stimulated Brillouin scattering in supersonic flowing plasmas by different forms of incident lasers

S S Ban(班帅帅), Q Wang(王清), Z J Liu(刘占军), C Y Zheng(郑春阳), X T He(贺贤土)
Chin. Phys. B, 2020, 29 (**9**): 095202. DOI: 10.1088/1674-1056/ab9c12

Generation of high quality ion beams through the stable radiation pressure acceleration of the near critical density target

Xue-Ren Hong(洪学仁), Wei-Jun Zhou(周伟军), Bai-Song Xie(谢柏松), Yang Yang(杨阳), Li Wang(王莉), Jian-Min Tian(田建民), Rong-An Tang(唐荣安), Wen-Shan Duan(段文山)
Chin. Phys. B, 2017, 26 (**6**): 065203. DOI: 10.1088/1674-1056/26/6/065203

Detailed calibration of the PI-LCX: 1300 high performance single photon counting hard x-ray CCD camera

Wei Hong(洪伟), Xian-Lun Wen(温贤伦), Lai Wei(魏来), Bin Zhu(朱斌), Yu-Chi Wu(吴玉迟), Ke-Gong Dong(董克攻), Chun-Ye Jiao(焦春晔), Bo Wu(伍波), Ying-Ling He(何颖玲), Fa-Qiang Zhang(张发强), Wei-Min Zhou(周维民), Yu-Qiu Gu(谷渝秋)
Chin. Phys. B, 2017, 26 (**2**): 025204. DOI: 10.1088/1674-1056/26/2/025204

Nonlinear mixing-based terahertz emission in inclined rippled density plasmas

K Gopal[1], A P Singh[1], and S Divya[2,†]

[1] *Rajdhani College, Department of Physics & Electronics, University of Delhi, New Delhi, India*

[2] *Computational Plasma Dynamics Laboratory, Rajdhani College, Department of Physics & Electronics, University of Delhi, New Delhi, India*

(Received 27 September 2022; revised manuscript received 7 November 2022; accepted manuscript online 8 December 2022)

We propose to investigate the THz field generation using nonlinear mixing mechanism of laser beat wave with inclined rippled density plasmas. Two laser pulses with frequencies (ω_1, ω_2) and wave vectors (k_1, k_2) co-propagate and resultant laser beat wave forms at beat frequency $(\omega_1 - \omega_2)$. Laser beat wave imparts a nonlinear force on the ambient electrons and pushes them outward with nonlinear velocity $v_{\rm NL}$. Coupling of induced density perturbation and nonlinear velocity $v_{\rm NL}$ generates nonlinear currents at laser beat frequency that further generates electromagnetic field $E_{(\omega_1-\omega_2)}$ in terahertz (THz) range. In the present scheme, density ripples are introduced at an angle with respect to laser propagation and flat Gaussian index (f) is introduced in laser field profile that transform curved top of Gaussian field envelope into flat top field envelope. The combined effect of flat laser pulses with inclined density ripples in plasmas shows 10-fold enhancement in THz field amplitude when flat-Gaussian index (f) varies from 1 to 4. Also, the THz field intensifies when density ripples inclination increases upto a certain angle and then decreases.

Keywords: terahertz, inclined ripple, flat laser, laser plasma interaction

PACS: 52.38.–r, 52.65.–y, 52.35.Mw **DOI:** 10.1088/1674-1056/aca9c9

1. Introduction

Electromagnetic radiations that lie in between the microwave and infrared range of EM wave spectrum are termed as terahertz radiations. Terahertz technology is capable of catering variety of applications spanning over a wide range from electronics to photonics.[1] For past few decades terahertz technology is continuously emerging and it has been served as an excellent radiation sources in particular for imaging purpose,[2] medical diagnosis,[3] and clinical applications.[4] Since, terahertz radiation does not ionize biomolecules rather terahertz energy spectrum matches with the characteristic energies of biomolecules and specially C–H–O bonds. Therefore, in medical diagnosis, terahertz radiation offers a significant advantage over x-rays due to the lower energy range of former while latter is harmful to vital tissues. Henceforth, it has been a great quest to the researchers across the globe to generate cost effective, table top tunable terahertz radiation of wider frequency and field range. In order to achieve this goal, several conventional schemes, *e.g.* optical rectification,[5] photoconductive antenna,[6,7] dielectrics,[8] monolayer graphene,[9] quantum cascade lasers,[10] have been proposed and investigated for terahertz radiation sources. Of all the above-mentioned generation schemes of terahertz radiation involve their benefits and drawbacks. There arise chances of material damage and breakdown of crystal, semiconductor, and dielectrics, when high power lasers are used. Plasma based schemes are at par with damage limit, preferably because plasma can sustain and easily handle highly energetic laser pulses as plasma by its own virtue is in ionized form that is electrically neutral and exhibits collective behavior. Also, the peak power of THz radiations can be enhanced with power of pulsed laser as laser technologies advances in future. Therefore, laser-plasma-based schemes for generation of THz radiations have attracted much interest since last two decades.

Hamster[11] and coworkers experimentally demonstrated generation of intense THz pulse from relativistic highly intense laser–plasma interaction via gaseous as well as solid targets. Most recently, decoherence effects of terahertz generation in solids under two-color femtosecond laser fields has been studied by Peng *et al.*[12] An intense laser pulse excites electrostatic plasma oscillations in underdense plasma; under ordinary condition, the dispersion relations of excited high amplitude electrostatic wakefield plasma oscillations do not match with electromagnetic radiation, however radiation does not emit. The linear-mode conversion (LMC) from laser wakefield to electromagnetic pulses (in THz range) can occur in inhomogeneous plasma under certain conditions is demonstrated by Sheng *et al.*[13] Terahertz pulses can also be obtained by interaction between laser wakefield and a static magnetic field in Cherenkov wake radiation mechanism.[14] Several research groups across the globe have investigated laser–plasma interaction[15] in view of generation of THz radiation by considering different kinds of inhomogeneous plasma[16,17] with

†Corresponding author. E-mail: dsingh@rajdhani.du.ac.in

© 2023 Chinese Physical Society and IOP Publishing Ltd

tailored lasers,[18] collisional plasma with super-Gaussian lasers,[19] and collisional anisotropic magnetized plasma.[20] Some groups have obtained Bessel terahertz pulses from mid infrared two color laser plasma filaments[21] and enhanced terahertz by fs laser fields assisted with sub-cycle pulses.[22] Most recent, Bessel terahertz pulses from superluminal laser plasma filaments have also been reported.[23] Also, Himani *et al.*[24] have investigated THz radiations where they considered the propagation of amplitude modulated Gaussian beam at modulation frequency in non-uniform plasma channel; they demonstrated that the self-focusing of modulated pulse significantly enhance the power of emitted THz radiations. Li and coworkers[25] in a recent study reported the creation of multi-frequency terahertz waves by optimized cascaded difference frequency generation. Also, the propagation of terahertz waves in nonuniform plasma slab under "electromagnetic window" is extensively studied by Li & Zhang.[26]

Another scheme of terahertz emission is governed by the nonlinear mixing of laser pulses which requires the energy momentum balance to achieve resonance for maximum transfer of energy from lasers to terahertz radiation using a nonlinear medium called as "plasma". In order to establish resonant transfer of energy for maximized terahertz field excitation, the density rippled plasma is being employed so that a tunable phase matching condition may be achieved. Such phase matching may also be attempted by the employment of magnetic wigglers[27] but magnetic field controlled phase matching is difficult to handle experimentally and even the range is poor. On the other hand, Singh & Malik[28] have applied external periodic electrostatic field and reported terahertz emission by achieving multiple resonances. Other groups[29] have observed significant enhancement in THz field amplitude with increasing value of electric field and also reported the changed polarization of produced THz radiations from linear to elliptical one. Most recently, intense low-noise terahertz generation have been reported by relativistic laser irradiating near-critical-density plasma by Zhang and coworkers.[30] Instead, a more probable and practical technique to achieve phase matching is to apply density ripples in plasma which can be created by different masked patterns or machining laser beams or by circular grating axicon assembly to focus the laser in a periodic manner.

In the present work, we study the generation of terahertz radiation by nonlinear optical mixing of two lasers of nearly varied frequency in the presence of inclined density ripples in cold plasma. We examine the effect of inclination of density ripple in plasma to ensure the resonant excitation of terahertz field by active control over phase matching condition. We also employ flat laser beam profile in place of normal distribution Gaussian pulse to see the effect of flatness of laser pulses on the mechanism of terahertz generation. The schematic diagram of the paper follows (see Fig. 1), after introduction in the first section, we discuss physical model in the second section using the above-mentioned laser–plasma arrangement. In the third section, results are discussed and conclusion is presented in the last section.

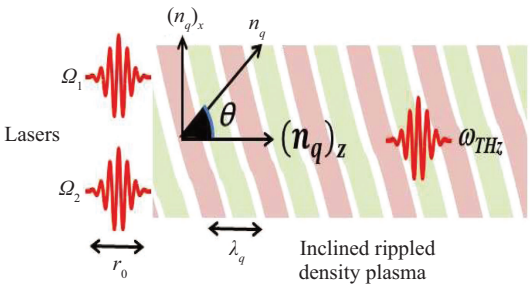


Fig. 1. The schematic diagram for nonlinear mixing mechanism in inclined density rippled plasma.

2. Physical model

Present physical model deals with the generation of the THz field during the laser beat wave interaction with the inclined rippled density plasma. Here, we consider two co-propagating laser pulses having electric field profile[31] as

$$\boldsymbol{E}_j = \hat{x} A_0 \exp[(y^2/r_0^2) f] \exp[\mathrm{i}(k_j z - \Omega_j t)], \tag{1}$$

where A_0 is the peak amplitude of the laser pulses, f is flat-Gaussian (FG) index, and r_0 is the laser spot size. Peak amplitude of the laser pulse changes from round top to flat top when flat-Gaussian index changes from $f = 1$–4.

Thus, the variation of the parameter 'f' induces the flatness in the laser field profile and therefore intensity redistribution takes place in space which significantly affects the laser–plasma interaction. Inhomogeneous plasma is considered in the form of inclined density ripples with respect to the laser propagation, therefore, plasma density is considered as[32]

$$n = n_0 + n_q, \quad n_q = n_{q0}\, \mathrm{e}^{\mathrm{i}(q_x x + q_z z)}, \tag{2}$$

where, ripple wave vector $\boldsymbol{q}$ is supposed to subtend an angle θ with respect to the laser propagation direction, $q = 2\pi/\lambda_q$, with λ_q being the ripple wave vector. Experimentally, laser machining is the process to form the density ripples during plasma density structure formation.[33] Inclusions of the density ripples conserve the extra momentum required for THz field generation.

Above-mentioned laser field profiles in Eq. (1) comprise electric field oscillations with varying peak amplitude that give rise to an inhomogeneous field in space. Plasma electrons attain oscillatory velocity $\boldsymbol{v}_j = e\boldsymbol{E}_j/m\mathrm{i}\Omega_j$ in laser field direction. Inhomogeneous electric field of the laser pulse imparts a

nonlinear ponderomotive force on plasma electrons expressed as follows:

$$\boldsymbol{F}_{\rm p} = -\frac{m}{2}(\boldsymbol{v}_j\cdot\nabla\boldsymbol{v}_j^* + \boldsymbol{v}_j^*\cdot\nabla\boldsymbol{v}_j) - \frac{e}{2c}(\boldsymbol{v}_j\times\boldsymbol{B}_j^* + \boldsymbol{v}_j^*\times\boldsymbol{B}_j), \tag{3}$$

where $v_j = e\boldsymbol{E}_j/m\mathrm{i}\Omega_j$ is the oscillatory velocity attained by plasma electrons in the influence of laser field. Ponderomotive force generates at laser beat frequency $(\Omega_1-\Omega_2)$ in case of the laser beat wave; therefore, other nonlinear terms, *e.g.*, $\boldsymbol{v}_1\times\boldsymbol{B}_1$ and $\boldsymbol{v}_2\times\boldsymbol{B}_2$ are neglected as they contribute at 2Ω frequency.[34] Dynamical equation of plasma electrons in the influence of the ponderomotive force can be expressed as $\partial\boldsymbol{v}_\Omega^{\rm NL}/\partial t = \boldsymbol{F}_{\rm p}/m$ that gives nonlinear velocity at laser beat frequency $(\Omega=\Omega_1-\Omega_2)$ as follows:

$$v_\Omega^{\rm NL} = \hat{z}\frac{\mathrm{e}^2(k_1-k_2)E_1E_2^*}{2m^2\Omega\Omega_1\Omega_2}, \tag{4}$$

where $\Omega=\Omega_1-\Omega_2$ lies in the terahertz range. Since the divergence of the nonlinear velocity is non-zero, it gives rise to nonlinear current density perturbation at $\Omega=\Omega_1-\Omega_2$ and k_1-k_2. Expression of the nonlinear density perturbation can be obtained from the continuity equation

$$\frac{\partial n_\Omega^{\rm NL}}{\partial t} + \nabla\cdot(n_0\boldsymbol{v}_\Omega^{\rm NL}) = 0,$$

and its solution is

$$n_\Omega^{\rm NL} = \frac{n_0\,\mathrm{e}^2(k_1-k_2)^2E_1E_2^*}{2m^2\Omega^2\Omega_1\Omega_2}. \tag{5}$$

Space charge field $\boldsymbol{E}_{\rm s} = \nabla\phi_{\rm s}$ is generated by the linear density perturbation and expressed as

$$n_\Omega^{\rm L} = (k_1-k_2)^2\chi_{\rm e}\phi_{\rm s}/(4\pi e),$$

where $\chi_{\rm e} = \Omega_{\rm p}^2/\Omega^2$ is the free electron susceptibility. Therefore, net space charge potential can be estimated using the Poisson's equation

$$\nabla^2\phi_{\rm s} = 4\pi e(n_\Omega^{\rm L} + n_\Omega^{\rm NL})$$

and expressed as

$$\phi_{\rm s} = \frac{eE_1E_2^*\Omega_{\rm p}^2}{2m\Omega_1\Omega_2(\Omega^2-\Omega_{\rm p}^2)}. \tag{6}$$

Net electron velocity due to ponderomotive force and the self-consistent field is

$$\boldsymbol{v}_\Omega = \frac{\boldsymbol{F}_{\rm p}+e\nabla\phi_{\rm s}}{m\mathrm{i}\Omega} = \frac{\mathrm{e}^2(\boldsymbol{k}_1-\boldsymbol{k}_2)\boldsymbol{E}_1\boldsymbol{E}_2^*\Omega}{2m^2\Omega_1\Omega_2(\Omega^2-\Omega_{\rm p}^2)}. \tag{7}$$

Coupling of nonlinear velocity of plasma electrons with density ripples produces an oscillatory nonlinear current

$$\boldsymbol{j}_\Omega^{\rm NL} = -en_q^*\boldsymbol{v}_\Omega/2$$

at beat frequency Ω, and wave-vector $\boldsymbol{k}=\boldsymbol{k}_1-\boldsymbol{k}_2-\boldsymbol{q}$, it can be expressed as

$$\boldsymbol{j}_\Omega^{\rm NL} = \hat{z}\frac{\mathrm{e}^3n_{q0}(\boldsymbol{k}_1-\boldsymbol{k}_2)\Omega\boldsymbol{E}_{01}\boldsymbol{E}_{02}^*\,\mathrm{e}^{\mathrm{i}[\Omega t-(k_1-k_2-q\cos\theta)z-(q\sin\theta)x]}}{4m^2\Omega_1\Omega_2(\Omega^2-\Omega_{\rm p}^2)}. \tag{8}$$

The THz field generated by nonlinear mixing mechanism can be estimated from the Maxwell wave equations that are derived from the third and fourth Maxwell's equations,[35]

$$\nabla^2\boldsymbol{E}_{\rm Thz} - \nabla(\nabla\cdot\boldsymbol{E}) - \frac{\partial^2\boldsymbol{E}}{\partial t^2} = -\frac{4\pi\mathrm{i}\Omega}{c^2}(\boldsymbol{j}_\Omega^{\rm L}+\boldsymbol{j}_\Omega^{\rm NL}),$$

where $\boldsymbol{j}_\Omega^{\rm L} = n_0\,\mathrm{e}^2\boldsymbol{E}/(m\mathrm{i}\Omega)$ is the linear current density due to self-consistent field E_Ω at Ω,k. Under the linearization process one can write $\partial/\partial t = -\mathrm{i}\Omega$, then the above wave equation takes the following form

$$\nabla^2\boldsymbol{E}_{\rm Thz} - \nabla(\nabla\cdot\boldsymbol{E}) + \frac{\Omega^2-\Omega_{\rm p}^2}{c^2}\boldsymbol{E}_{\rm Thz} = \frac{4\pi\mathrm{i}\Omega}{c^2}\boldsymbol{j}_\Omega^{\rm NL}. \tag{9}$$

Taking divergence of the above equation, one can obtain $\nabla\boldsymbol{E}_{\rm Thz} = -4\pi\mathrm{i}\Omega\cdot\nabla\boldsymbol{j}_\Omega^{\rm NL}/(\Omega^2-\Omega_{\rm p})^2$. Hence, final wave equation can be reduced as

$$\nabla^2\boldsymbol{E}_{\rm Thz} + \frac{(\Omega^2-\Omega_{\rm p}^2)}{c^2}\boldsymbol{E}_{\rm Thz} = -\frac{4\pi\mathrm{i}\Omega}{c^2}\boldsymbol{j}_\Omega^{\rm NL}\times\left[\boldsymbol{j}_\Omega^{\rm NL} + \frac{c^2}{(\Omega^2-\Omega_{\rm p}^2)}\nabla(\nabla\cdot\boldsymbol{j}_\Omega^{\rm NL})\right]. \tag{10}$$

In the present numerical calculation, the laser pulse is considered non-evolutionary; one can write ∇ as $\mathrm{i}k_{\rm THz}$, where $\boldsymbol{k}_{\rm THz} = \boldsymbol{k}_1-\boldsymbol{k}_2-\boldsymbol{q}$ and the above equation can be written as

$$\left[-k_{\rm THz}^2 + \frac{(\Omega^2-\Omega_{\rm p}^2)}{c^2}\right]\boldsymbol{E}_\Omega = -\left(\frac{4\pi\mathrm{i}\Omega}{c^2}\right)\left[\boldsymbol{j}_\Omega^{\rm NL} - \frac{c^2}{(\Omega^2-\Omega_{\rm p}^2)}\boldsymbol{k}_{\rm THz}(\boldsymbol{K}_{\rm THz}\cdot\boldsymbol{j}_\Omega^{\rm NL})\right]. \tag{11}$$

The phase matching condition can be expressed as $k_{\rm THz}^2 = (\Omega^2 - \Omega_{\rm p}^2)/c^2$. In the case of finite spot size, the THz field will also be observed in other than the spot size region after traveling some distance in plasma of the order $r_0/\sin\theta_\Omega$, where θ_Ω is the angle between THz wave vector $k_{\rm THz}$ and z axis,

$$\theta_\Omega \tan^{-1}\left(\frac{q\sin\theta}{k_1 - k_2 - q\cos\theta}\right).$$

Also, the phase matching condition demands

$$q = \frac{\Omega}{c}\left[\cos\theta - \left(\cos^2\theta - \frac{\Omega_{\rm p}^2}{\Omega^2}\right)^{1/2}\right].$$

The THz wave equation under the inclusion of the THz wave angle and finite size approximation takes the form as

$$\nabla^2 \boldsymbol{E}_\Omega + \frac{(\Omega^2 - \Omega_{\rm p}^2)}{c^2}\boldsymbol{E}_\Omega = R_0\, {\rm e}^{-r^2/r_0^2}\, {\rm e}^{-{\rm i}[\Omega t - (k_1 - k_2 - q\cos\theta)z - (q\sin\theta)x]}, \tag{12}$$

where $R_0 = R_{0z}\hat{z} + R_{0x}\hat{x}$ with

$$R_{0z} = -\frac{{\rm i}\pi n_{q0}\,{\rm e}^3\Omega^2(k_1 - k_2)A_{01}A_{02}^*}{m^2c^2\Omega_1\Omega_2(\Omega^2 - \Omega_{\rm p}^2)} \times \left(1 - \frac{c^2(k_1 - k_2 - q\cos\theta)^2}{\Omega^2 - \Omega_{\rm p}^2}\right),$$
$$R_{0x} = -\frac{{\rm i}\pi n_{q0}\,{\rm e}^3\Omega^2(k_1 - k_2)A_{01}A_{02}^*}{m^2c^2\Omega_1\Omega_2(\Omega^2 - \Omega_{\rm p}^2)} \times \left(\frac{c^2 q\sin\theta(k_1 - k_2 - q\cos\theta)^2}{\Omega^2 - \Omega_{\rm p}^2}\right).$$

The solution of wave equation can be estimated under the rotation of coordinate system clockwise by an angle θ_Ω to align the new z axis along γ, *i.e.*, parallel to $k_{\rm THz}$, and x axis along α, *i.e.*, perpendicular to $k_{\rm THz}$. Therefore, new coordinates can be expressed as $\gamma = z\cos\theta_\Omega - x\sin\theta_\Omega$ and $\alpha = z\sin\theta_\Omega + x\cos\theta_\Omega$.[36] Similarly, γ and α components of R_0 can be written as $R_{0\gamma} = R_{0z}\cos\theta_\Omega - R_{0x}\sin\theta_\Omega$ and $R_{0\alpha} = R_{0z}\sin\theta_\Omega + R_{0x}\cos\theta_\Omega$. Since the transverse component $R_{0\alpha}$ of R_0 is relevant to THz field generation; it can be expressed as

$$R_{0\alpha} = \frac{{\rm i}\pi n_{q0}\,{\rm e}^3\Omega^2(k_1 - k_2)A_{01}A_{02}^*}{m^2c^2\Omega_1\Omega_2(\Omega^2 - \Omega_{\rm p}^2)} \times \left[\left(1 - \frac{c^2(k_1 - k_2 - q\cos\theta)^2}{\Omega^2 - \Omega_{\rm p}^2}\right)\sin\theta_\Omega + \left(\frac{c^2 q\sin\theta(k_1 - k_2 - q\cos\theta)^2}{\Omega^2 - \Omega_{\rm p}^2}\right)\cos\theta_\Omega\right]. \tag{13}$$

Equation (13) takes form in rotated coordinate system as

$$\frac{\partial^2}{\partial\gamma^2}E_{\Omega\alpha} + \frac{\partial^2}{\partial\alpha^2}E_{\Omega\alpha} + \frac{\partial^2}{\partial y^2}E_{\Omega\alpha} + \frac{(\Omega^2 - \Omega_{\rm p}^2)}{c^2}E_{\Omega\alpha} = R_{0\alpha}\,{\rm e}^{-r^2/r_0^2}\,{\rm e}^{-{\rm i}[\Omega t - (k_1 - k_2 - q\cos\theta)z - (q\sin\theta)x]}, \tag{14}$$

where $r^2 = y^2 + (\alpha\cos\theta_\Omega - \gamma\sin\theta_\Omega)^2$ and $k_{\rm THz} = (k_1 - k_2 - q\cos\theta)\cos\theta_\Omega + (q\sin\theta)\sin\theta_\Omega$. The dependence of $E_{\Omega\alpha}$ on γ is stronger than that on α and y. Therefore, the solution of equation can be given by $\boldsymbol{E}_{\Omega\alpha} = E_{0\Omega}\,{\rm e}^{-{\rm i}(\Omega t - k_{\rm THz}\gamma)}$. Equation (14) is reduced to

$$2{\rm i}k_{\rm THz}\frac{\partial E_\Omega}{\partial\gamma} + \frac{\partial^2 E_\Omega}{\partial\gamma^2} + \left(-k_{\rm THz}^2 + \frac{\Omega^2 - \Omega_{\rm p}^2}{c^2}\right)E_\Omega = R_{0\alpha}\,{\rm e}^{(-y^2 + (\alpha\cos\theta_\Omega - \gamma\sin\theta_\Omega)^2)/r_0^2}. \tag{15}$$

With the exact phase matching condition, the above equation is reduced to

$$\frac{\partial E_\Omega}{\partial\gamma} = \frac{R_{0\alpha}\,{\rm e}^{(-y^2 + (\alpha\cos\theta_\Omega - \gamma\sin\theta_\Omega)^2)/r_0^2}}{2{\rm i}k_{\rm THz}}. \tag{16}$$

Hence, the final expression of normalized THz field amplitude can be expressed as

$$\left|\frac{E_{0\Omega}}{A_{01}}\right|_x = \frac{n_{q0}}{4n_0}\frac{\Omega'^2|v_{02}'^*|}{\Omega_1'(\Omega'^2 - 1)^2}\left[-\frac{4fy'}{r_0'^2}\left(\frac{y'^2}{r_0'^2}\right)^{f-1}\right]\exp\left[-2\left(\frac{y'^2}{r_0'^2}\right)^f\right]\cdot\frac{1}{(1 - \cos(\theta - \theta_\Omega))\left[\cos\theta - \left(\cos^2\theta - \Omega_{\rm p}^2/\Omega^2\right)^{1/2}\right]}. \tag{17}$$

3. Results and discussion

Here, we discuss the numerical results related to the THz field generation, when laser beat wave interacts with inclined rippled plasmas under the phase matching condition. FG-index (f) introduces flatness in laser beam profile that changes the laser intensity distribution in space, therefore, interaction of laser beat wave with ambient plasma electrons changes significantly. Numerical simulations are performed for laser pulses having wavelength (λ_1) of 800 nm and angular fre-

quency $\Omega_1 = 2.34 \times 10^{13}$ rad/s. The frequency of the second laser is chosen as $\Omega_1 - \Omega_2 = \Omega_T$. Laser strength parameter $a_j = eA_{0j}/(m\Omega_{0j})$ is chosen as 0.1, 0.2, and 0.3, where A_{0j} is the amplitude of the laser pulse and the corresponding intensity lies in the range of 10^{16} W/cm^2. The plasma density is chosen in the range 10^{16} cm^{-3}–10^{17} cm^{-3}. Density ripples are introduced with modulation of plasma electrons density of 10%, 20%, 30%, and 40% with respect to the equilibrium plasma density (n_0). Density ripples are introduced at an angle θ with respect to the laser propagation and, also, THz field is observed at an angle θ_Ω with respect to the laser propagation. Normalized THz field is estimated in present numerical calculations with respect to THz frequency, inclination angle of density ripples, and the amplitude of the density ripples for different FG-index (f). Figure 2 describes the generated electromagnetic field in the THz range with respect to the THz frequency for different values of the FG-index (f). It shows the importance of pulse flatness that how it may control the terahertz field energy.

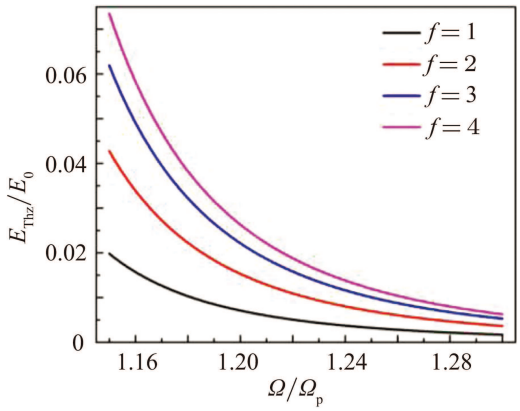


Fig. 2. Variation of the THz field amplitude with normalized frequency for varying FG-index (f). Laser strength parameter $a_j = eE_{0j}/(m\Omega_{0j})$ is chosen as 0.1, the laser intensity is 10^{16} W/cm^2 and the plasma density is 10^{17} cm^{-3}. Density ripples are inclined at $\pi/6$ with respect to the laser propagation.

Terahertz field enhances for higher value of FG-index "$f = 4$"as compared to lower FG-index $f = 1$, $f = 2$, and $f = 3$ respectively. Generated THz field attains peak value near the resonance and it decreases sharply away from the resonance condition. Maximum laser beat wave energy transfers into the THz field at resonance. The THz field amplitude is observed to increase with the value of FG index increasing, the gradient force imparted by the laser beat wave is enhanced with FG-index (f) increasing and thus further improving the generated current density. Extra current component is generated with inclined density ripples (mentioned in the physical model) that implies the enhancement in the THz field amplitude. The present results show that the intensity of THz field is increased by 10-fold in comparison with the intensity previously reported THz field,[37] which is of the order 10^{-3} for curved-Gaussian laser with density ripples in laser propagation direction in electron–ion plasmas. In other research, Divya[39] has studied the influence of hot electrons on optical excitation of terahertz radiation by the beating of super-Gaussian lasers in electron–positron collisional plasma and found decayed amplitude of the THz field due to thermal effects. Comparatively, the present scheme of inclined ripples in plasma for propagating flat Gaussian laser offers better enhancement in the THz field amplitude than previously reported study. Considering the generation mechanism of the THz radiation, the present approach will be a good choice to deal with collisional plasma with thermal effects.

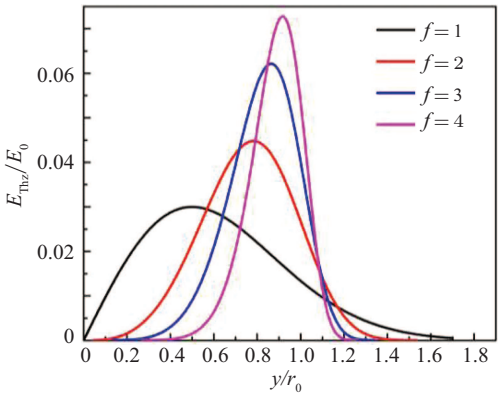


Fig. 3. The variation of the THz field amplitude with transverse distance for different FG-indexes (f). Laser strength parameter $a_j = eE_{0j}/(m\Omega_{0j})$ is chosen as 0.1, the laser intensity is 10^{16} W/cm^2 and the plasma density is 10^{17} cm^{-3}, and $\Omega/\Omega_T = 1.16$.

Also, the present physical model reports the enhanced THz field with previously reported studies of the THz field generation in semiconductor plasmas[38] and the mixture of nanoparticles and argon gas.[35] Figure 3 depicts the variation of the normalized terahertz field amplitude with normalized transverse distance for different FG-indices (f) of lasers. One can see obvious results of significant enhancement in terahertz field for $f = 4$, showing subsequently decays for lower values of "f", *i.e.*, large values of FG-index (f) corresponding to the flat top lasers provide better enhancement than lower flat index parameter which is more alike Gaussian pulse. If we analyze the energy distribution of the terahertz pulse through Fig. 3, it is more symmetric for $f = 4$ and least symmetric for $f = 1$. This symmetric energy distribution may be regarded as the focal spot of the emitted terahertz. Thus larger flat index provides tight focused terahertz radiation. Since, the present approach to the generation of the terahertz radiation mainly deals with the active control of mechanism by inclined density ripple. In Fig. 4, the variations of the normalized terahertz field with the normalized ripple density for different FG-indices of lasers are discussed.

Obviously, the ripples in the plasma density are found to support this mechanism via proper phase matching, which leads to the conservation of momentum in nonlinear mixing mechanism, and finally leads to the resonance condition,

where the maximum laser energy is converted into the THz field energy. Hence, the THz amplitude reaches a peak value at resonance and decreases with distance from the resonance increasing. Whereas, in uniform density plasma it becomes difficult to achieve resonance via exact phase matching experimentally. The number of electrons is enhanceed in laser–plasma interaction as density ripple amplitude increases and therefore, current density increases, resulting in intensified THz emission. Also, flat Gaussian pulses affect the stronger ponderomotive force due to their large intensity gradient, creating a larger nonlinear velocity to free electrons and hence amplifying the nonlinear current density during laser–plasma interaction in nonlinear mixing mechanism.

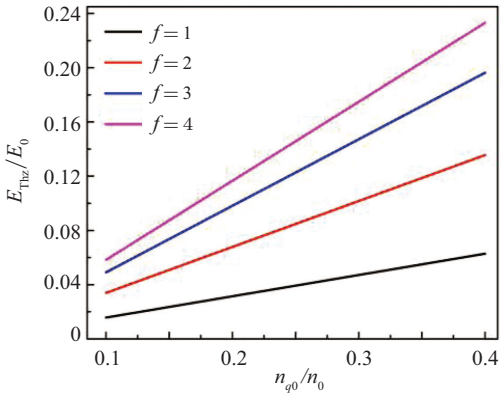


Fig. 4. Variations of the THz field amplitude with density ripple amplitude for different FG-indexes (f). Laser strength parameter $a_j = eE_{0j}/(m\Omega_{0j})$ is chosen as 0.1, the laser intensity is 10^{16} W/cm^2, the plasma density is 10^{17} cm^{-3}, and $\Omega/\Omega_T = 1.16$.

Figure 5 shows the distribution of the THz field with respect to the density ripple angle for different flat indexes. It is evident from the results that the THz field attains peak value at an inclination of 60° relative to the laser propagation and then decreases successively. Further, figures 5(b)–5(d) show four-fold enhancement in generated THz field energy when FI parameter (f) varies from $f = 1$ to $f = 4$. It is important to report that the angular distribution of the THz field energy is the same as that with respect to inclined rippled plasmas for varying flat-Gaussian index (f), so that the THz polarisation ellipse will not change with the flat-Gaussian index. Therefore, the combined effect of the laser pulse flatness and density ripple inclination produces intensified THz radiations in comparison with previously reported arrangement of laser–plasma parameters for THz field generation. Also, the efficiency[19] of the present physical mechanism can be described as the ratio $\eta = W_{\rm Thz}/W_{\rm L}$, where

$$W_{\rm Thz} = \frac{1}{2}\varepsilon\langle E_{\rm Thz}^2\rangle = \frac{1}{2}\varepsilon_0\int_{-\infty}^{\infty} E_{\rm Thz}^2\,{\rm d}y$$

is the average electromagnetic energy density for emitted THz emission and $W_{\rm L} = \frac{1}{2}\varepsilon_0\langle E_{\rm L}^2\rangle = \frac{1}{2}\varepsilon_0\int_{-\infty}^{\infty} E_{\rm L}^2\,{\rm d}y$ is the average electromagnetic energy density for the incident laser. THz field efficiency (η) is estimated numerically in the range of 10^{-3}–10^{-4} for varying values of the FG-index (f) for an optimized inclination of the density ripples that is significantly higher than that from previously reported mechanism[11,38] of the THz emission.

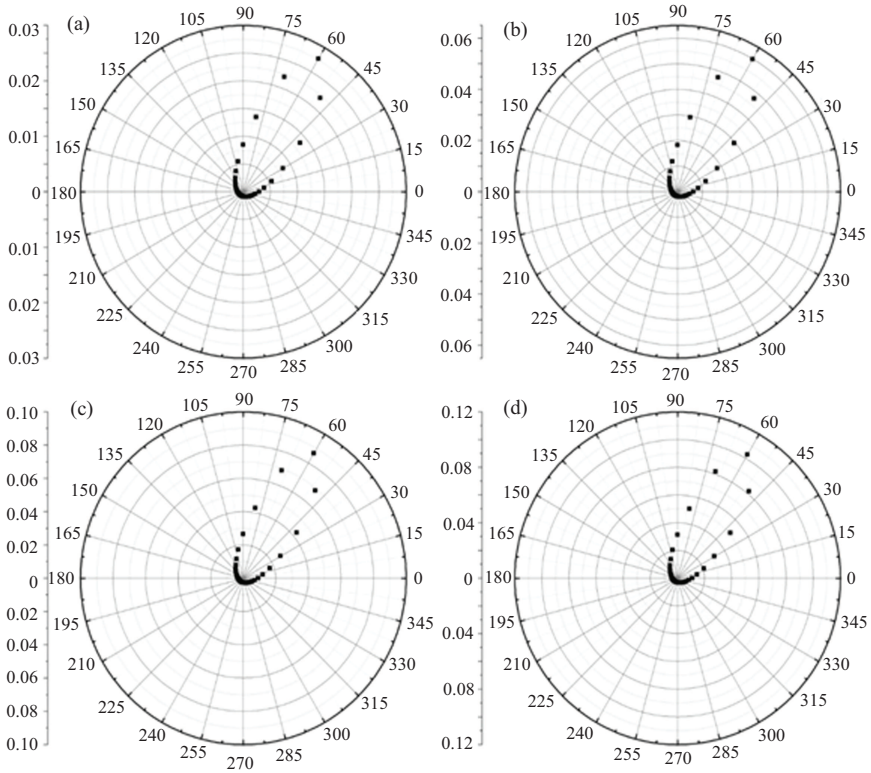


Fig. 5. THz field distributions with respect to density ripple angle for different values of the flat-index. Laser plasma parameters are considered to be the same as in previous figures.

4. Conclusion

The THz field generation is reported by using the nonlinear mixing mechanism in laser–plasma interactions, where inclined density ripples and laser pulse flatness are proposed as controlling parameters. The THz field attains a peak value at resonance and decreases sharply away from the resonance. The THz field energy reaches a peak value as inclination of the density ripples increases upto a certain value and then it starts to decrease. Also, the field amplitude is observed to increase significantly with the value of the FG-index (f) increasing. Therefore, the THz field with a desired frequency and amplitude can be obtained by tuning the laser and plasma property. The present study can also be extended to the case in presence of external magnetic field that would act as an additional controlling parameter, for it will affect the dynamics of plasma electrons during interactions with lasers.

Acknowledgement

The authors acknowledge Rajdhani College, University of Delhi, their parent institution for providing adequate resources to conduct this research.

References

[1] Dragoman D and Dragoman M 2004 *Progress in Quantum Electron* **28** 1
[2] Mittleman D M, Jacobsen R H and Nuss M C 1996 *IEEE J. Select. Top. Quantum Electron.* **2** 679
[3] Chen M, Wang Y, Wang Y and Li L 2022 *Front. Phys.* **10** 855623
[4] Son J H, Oh J S and Cheon H 2019 *J. Appl. Phys.* **125** 190901
[5] Bhasin L and Tripathi V K 2009 *Phys. Plasmas* **16** 103105
[6] Shi W, Wang Z, Hou L, Wang H, Wu M and Li C A 2021 *Front. Phys.* **9** 751128
[7] Liu X, Meng Q H, Ding J, Bai, Wang J H, Zhang C, Su B and Zhang C L 2022 *Chin. Phys. B* **31** 028701
[8] Lan C, Bi K, Li B, Zhao Y and Qu Z 2017 *Opt. Express* **25** 29155
[9] Guan Z, Wang G L, Zhang L, Jiao Z H, Zhao S F and Zhou X X 2021 *Chin. Phys. Lett.* **38** 054201
[10] Szymański M, Szerling A and Kosiel K 2015 *Opt. Quantum Electron.* **47** 843
[11] Hamster H, Sullivan A, Gordon S, White W and Falcone R W 1993 *Phys. Rev. Lett.* **71** 2725
[12] Peng Q, Peng Z, Lang Y, Zhu Y, Zhang D, Lü Z and Zhao Z 2022 *Chin. Phys. Lett.* **39** 053301
[13] Sheng Z M, Mima K, Zhang J and Sanuki H 2005 *Phys. Rev. Lett.* **94** 095003
[14] Yoshii J, Lai C H, Katsouleas T, Joshi C and Mori W B 1997 *Phys. Rev. Lett.* **79** 4194
[15] Li Y T, Wang W M, Li C and Sheng Z M 2012 *Chin. Phys. B* **21** 095203
[16] Wu H C, Meyer-Ter-Vehn J, Ruhl H and Sheng Z M 2011 *Phys. Rev. E* **83** 036407
[17] Rizaev G E, Seleznev L V, Mokrousova D V, Pushkarev D V and Ionin A A 2022 *Opt. Lett.* **47** 5917
[18] Sheng W, Tang F, Zhang Z, Chen Y, Peng X Y and Sheng Z M 2011 *Opt. Express* **29** 8676
[19] Singh D and Malik H K 2014 *Phys. Plasmas* **21** 083105
[20] Singh D and Malik H K 2015 *Plasma Sources Sci. Technology* **24** 045001
[21] Koulouklidis A D, Gollner C, Shumakova V, *et al.* 2020 *Nat. Commun.* **11** 292
[22] Shu X F, Yu C X and Liu J 2019 *Opt. Express* **27** 7751
[23] Zhang Z, Zhang J, Chen Y, Xia T, Wang L, Han B, He F, Sheng Z and Zhang J 2022 *Ultrafast Science* **2022** 9870325
[24] Juneja H, Chauhan P and Panwar A 2022 *Optik* **268** 169791
[25] Li Z Y, Zhao J, Yuan S, Jiao B Z, Bing P B, Zhang H T, Chen Z L, Tan L and Yao J Q 2022 *Chin. Phys. B* **31** 044205
[26] Li H, Zhang Z P and Yang X 2022 *Chin. Phys. B* **31** 035202
[27] Kumar M and Tripathi V K 2012 *Phys. Plasmas* **19** 073109
[28] Singh D and Malik H K 2020 *Phys. Rev. E* **101** 043207
[29] Li M, Li A Y, He B Q, Yuan S and Zeng H P 2016 *Chin. Phys. B* **25** 044209
[30] Zhang S, Zhou W, Yin Y, Zou D, Zhao N, Xie D and Zhuo H 2022 *Chin. Phys. B* **32** 035201
[31] Gillen-Christandl K, Gillen G D, Piotrowicz M J and Saffman M 2016 *Appl. Phys. B* **122** 1
[32] Pathak V B, Dahiya D and Tripathi V K 2009 *J. Appl. Phys.* **105** 013315
[33] Pai C H, Huang S Y, Kuo C C, Lin M W, Wang J and Chen S Y 2005 *Phys. Plasmas* **12** 070707
[34] Bhasin L and Tripathi V K 2011 *Phys. Plasmas* **18** 123106
[35] Varshney P, Singh A P, Kundu M and Gopal K 2022 *Opt. Quantum Electron.* **54** 222
[36] Arfken G and Weber H 2005 *Mathematical Methods for Physicists*, 6th edn. (Boston: Elsevier AP)
[37] Malik A K, Malik H K and Nishida Y 2011 *Phys. Lett. A* **375** 1191
[38] Varshney P, Singh A P, Upadhyaay A, Kundu M and Gopal K 2022 *Optik* **250** 168353
[39] Divya S 2020 *Plasma Res. Express* **2** 045003